

Isolation of Neoclassical Toroidal Viscosity Profile Under Varied Plasma and 3D Field Conditions in Low and Medium Aspect Ratio Tokamaks

S.A. Sabbagh¹, Y.S. Park¹, R.E. Bell², J. Kim³, J. Ko³, W.H. Ko³, K.C. Shaing⁴, Y. Sun⁵, B. LeBlanc², S.G. Lee³, J. Lee³, J.W. Berkery¹, S.P. Gerhardt², S.H. Hahn³, Y. In³, Y.M. Jeon³, Y.K. Oh³, J.W. Yoo³

¹Department of Applied Physics, Columbia University, New York, NY, USA

²Princeton Plasma Physics Laboratory, Princeton University, Princeton, NJ, USA

³National Fusion Research Institute, Daejeon, Republic of Korea

⁴National Cheng Kung University, Tainan, Taiwan

⁵ASIPP, Hefei Anhui, China

E-mail contact of main author: sabbagh@pppl.gov

Abstract. The phenomenon of Neoclassical Toroidal Viscosity (NTV) due to non-ambipolar particle diffusion occurs in tokamaks due to low magnitude ($\delta\mathbf{B}/B_0 \sim O(10^{-3})$) three-dimensional (3D) applied fields, is often used for positive purposes including alteration of the plasma rotation profile, ω_ϕ , to stabilize MHD modes and for ELM suppression. As ITER and future devices will use 3D fields for these purposes, it is important to understand NTV effects over key plasma and 3D field variations. The present work analyzes and examines NTV in two tokamak devices of significantly different aspect ratio. This new and unique collection of data allows testing of NTV theory over a broad range of important plasma variations including aspect ratio, q_{95} , collisionality, temperature, normalized gyroradius, plasma rotation speed and profile, as well as applied 3D field strength and spectrum in both devices. Isolation of the NTV torque profile, T_{NTV} , is accomplished by applying the 3D magnetic field faster than the plasma momentum diffusion time. A new database was generated in a dedicated joint international experiment to measure the NTV profile this way for the first time in the KSTAR superconducting tokamak at medium aspect ratio ($A \sim 3.5$). These results are compared with new analysis of complementary experimental results from the extensive NTV database of low aspect ratio ($A \sim 1.3$) NSTX plasmas. The NSTX experiments yield unique information in plasmas with computed displacements smaller than the ion banana width, showing that finite-orbit effects will average T_{NTV} over such spatial scales. In KSTAR, six different 3D field spectra were run, including dominantly $n = 2$, $n = 1$ field pitch-aligned, $n = 1$ field pitch non-aligned configurations, and their superposition. As expected by theory, the measured rotation profile change due to the 3D field, $\Delta\omega_\phi$, does not change sign, and is close to zero at the plasma boundary. All cases show broader $\Delta\omega_\phi$ than found in NSTX. The change to the relative pitch alignment of the applied 3D field yielded a clear and unexpected result: the non-pitch-aligned field configuration produced a stronger change to the ω_ϕ profile than the pitch-aligned case. The $\Delta\omega_\phi$ is global and non-resonant, with no strong indication of localized resonant effects, similar to NSTX results in different field configurations. The NTV offset rotation profile is directly measured and studied in KSTAR, showing strong controlled rotation in the co- I_p direction at high T_e , and large increases (factor of 15) in the rotation shear in the outer plasma.

1. Introduction

The phenomenon of Neoclassical Toroidal Viscosity (NTV) due to non-ambipolar particle diffusion in a three-dimensional (3D) field has been proposed in theory [1], with the first quantitative validation by experiment [2] performed a decade ago. The effect has been used for positive purposes in tokamak experiments, including alteration of the plasma rotation profile, ω_ϕ (both the velocity and shear) using low magnitude ($\delta\mathbf{B}/B_0 \sim O(10^{-3})$) 3D fields. This ω_ϕ profile alteration can strongly affect the stability of disruption-inducing modes in tokamak plasmas, such as neoclassical tearing modes and resistive wall modes [3]. These, and other uses of 3D fields in tokamaks (i.e. suppression of ELMs and Alfvénic modes), benefit from broader experimental investigations of the dependence of NTV on key plasma parameters and 3D field spectra [4-6]. This understanding is especially important to

accurately extrapolate NTV effects to low collisionality plasmas in ITER when using 3D fields.

With the quantitative validation of NTV theory long established and comprehensively reviewed [7], recent research aims to investigate key aspects of NTV for further positive use in present and future tokamaks. The overall objective of the controlled use of NTV is to alter the plasma rotation profile, including use as an active feedback actuator [8]. This research can be divided into two general classes of plasmas (a) rapidly rotating, and (b) slowly rotating, which typically utilize different experimental techniques. In the former, predominantly non-resonant fields are applied to allow plasma rotation profile alteration by reducing rotation without causing mode locking. Further key NTV research in such plasmas includes how various applied 3D field spectra and plasma collisionality (temperature) can alter the rotation braking profile. In the latter case, the more general understanding and experimental verification of the NTV offset rotation profile is needed. The present paper addresses these two research areas in sections 2 and 3.

2. Isolation of NTV torque profile and comparison to theory in rotating plasmas

The present work quantitatively analyzes and compares NTV observed in two tokamak devices of significantly different aspect ratio. This new and unique collection of data allows testing of NTV theory over a broad scope of important plasma variations including aspect ratio, q_{95} , collisionality, temperature, normalized gyroradius ρ^* , plasma rotation speed and profile, as well as applied 3D field strength and spectrum in both devices. First, a new database was generated in a dedicated joint international experiment to isolate and measure the NTV profile for the first time in the KSTAR superconducting tokamak at medium aspect ratio ($A \sim 3.5$). Over 360 different variations of the parameters mentioned above were produced from this experiment alone. These results are compared with new analysis of complementary experimental results from the extensive NTV database of low aspect ratio ($A \sim 1.3$) National Spherical Torus Experiment (NSTX) plasmas.

2.1. Experimental aspects of non-resonant NTV in NSTX

Isolation of the NTV torque profile, T_{NTV} , is accomplished experimentally by applying the 3D magnetic field faster than the momentum diffusion time of the plasma, yielding a perturbation equation that balances the experimentally measured dL/dt profile against the theoretical T_{NTV} [2]. Figure 1 shows a full quantitative comparison of these profiles in NSTX, with T_{NTV} using a plasma response consistent with the applied 3D field (often used in theoretical calculations of T_{NTV}), emphasizing the comparison to the ion T_{NTV} profile averaged over the banana width, which as shown more accurately matches the measured dL/dt profile. Experiments at the low aspect ratio and high q of NSTX yield unique information in this regard, as the maximum computed theoretical plasma displacement $|\xi| = 0.3\text{cm}$ is smaller than the ion banana width, showing that finite-orbit effects will average T_{NTV} over such spatial scales, as recently examined theoretically [9]. The computed magnetic field used to compute T_{NTV} includes full detail of the coils in 3D and retains the full toroidal, n , and poloidal spectral decomposition in the calculations. A change in L is not found outside of error bars in the core of NSTX plasmas for analysis intervals much less than the momentum diffusion time. In contrast, measurements of L at later times clearly show diffusion of the NTV toward the core, spoiling the measured

T_{NTV} profile isolation. This emphasizes the importance of the experimental approach used here in isolating T_{NTV} .

2.2. Experimental aspects of non-resonant NTV in KSTAR

The KSTAR experiment provides both unique results and key comparisons to the NSTX data. The large database was created in a single experiment by leveraging the long pulse (20 second plasma duration) and new fast power supply capability (IPS) of the device that allowed up to 18 experimental data points per pulse in 20 discharges. Six different 3D field spectra were run, which included dominantly $n = 2$, $n = 1$ field pitch-aligned, $n = 1$ field pitch non-aligned configurations, and the superposition of these $n = 2$ and $n = 1$ configurations. Several key

plasma parameters were varied in the study including the applied 3D field strength, plasma collisionality (via divertor gas injection), plasma rotation speed and profile, T_i up to 3 keV, and $5.0 < q_{95} < 8.2$. Figure 2 shows the experimental evolution of the ω_ϕ profile (error bars shown) as measured by charge exchange spectroscopy (CES) diagnosis before and after the application of three primary 3D field spectra, isolating the non-resonant T_{NTV} profile. Measurements showed that strong resonant MHD modes were absent. As expected by theory, the measured rotation profile change due to the 3D field, $\Delta\omega_\phi$ (Fig. 2, bottom row) does not change sign, and is close to zero at the plasma boundary. All cases show broader $\Delta\omega_\phi$ (which represents the measured T_{NTV}) than found in NSTX, which is thought to be caused by the closer proximity of the coils to the plasma. The ability to change the relative pitch alignment of the applied 3D field to the equilibrium field adds a new capability compared to NSTX,

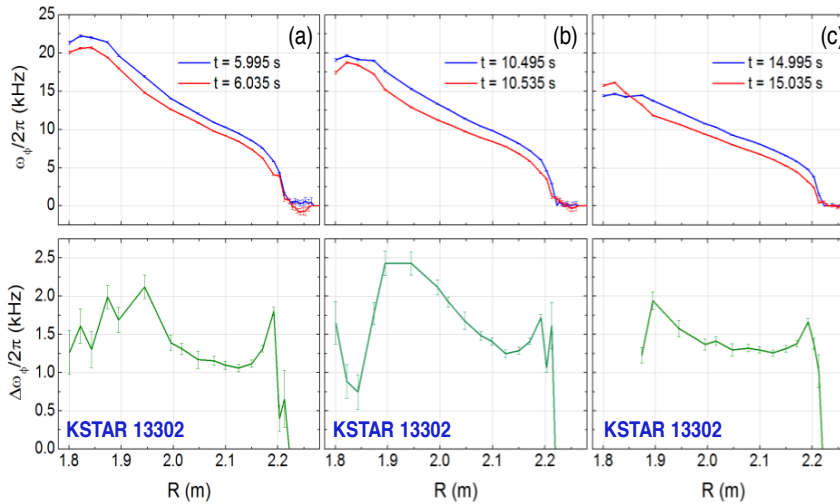


FIG. 2. Rotation profile alteration in KSTAR using (a) $n = 2$, (b) $n = 1$ pitch non-aligned, and (c) $n = 1$ pitch aligned 3D field configurations.

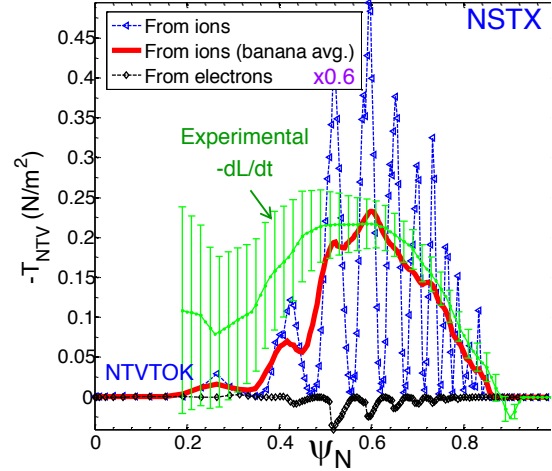


FIG. 1. T_{NTV} profile components for an $n = 3$ field configuration in NSTX ($\times 0.6$) computed for (i) ions using “vacuum field assumption”, (ii) ions using banana width-averaging, (iii) electrons. The measured ($-dL/dt$) profile is shown in green.

yielding a clear and unexpected result: the non-pitch-aligned field configuration produces a stronger change to the ω_ϕ profile than the pitch-aligned case. The pitch-aligned field was expected to yield larger T_{NTV} as the amplification of δB by the plasma should be stronger in this configuration. Further analysis will

determine the reason. The $\Delta\omega_\phi$ is global and non-resonant, with no strong indication of localized resonant effects, similar to NSTX results in different field configurations. The full analysis of the experimental and theoretical T_{NTV} profiles for KSTAR (analogous to the NSTX analysis (FIG. 1)) is underway. While this analysis is required for a quantitative conclusion, the NTV magnitude presently appears to be understood by simple superposition of the separate applied 3D field spectra.

3. Direct measurement of the NTV offset rotation profile in slowly rotating plasmas

Plasma rotation provides improved stability and confinement in contemporary tokamak plasmas utilizing unbalanced neutral beam injection. However, tokamak devices aiming to produce high fusion power output, including ITER, are expected to rotate much more slowly due to relatively small levels of momentum injection and larger plasma mass compared to present machines. Therefore methods of producing and altering plasma rotation on these devices are highly desired. Understanding how plasmas intrinsically rotate is of primary interest to confidently extrapolate this effect to ITER-scale plasmas as it may provide significant rotation. NTV physics also provides the potential for providing a form of intrinsic rotation in tokamaks such as ITER that can apply low-level non-axisymmetric fields to the plasma. This effect, typically referred to as the NTV “offset rotation” in the literature [6,7] may supplement other forms of plasma intrinsic rotation, or potentially provide the main rotation. The effect also has the potential of providing significant rotation shear in the plasma, a profile characteristic that is generally stabilizing for MHD modes. An important advantage of this effect is that it is controllable by varying the strength of the non-axisymmetric field. If sufficiently strong, this rotation and its shear could provide stabilization and improved performance in ITER and future devices.

Research to date has identified this affect in the DIII-D tokamak [10] with evidence of it also noted in experiments on TCV [11], yet important questions remain. In the DIII-D study, the total injected NBI torque, T_{NBI} , was attempted to be kept low to measure the offset rotation by making best efforts to balance the torque of the injected sources, but it is not possible to do this exactly for the entire profile, even if the NBI is set up to provide zero global net input torque. Both the NBI and NTV torques have radial profiles (especially important to determine flow shear), so aiming to have global net input torque of zero is not sufficient to ensure zero NBI torque across the plasma radius. Since the local NBI torque at a given point along the plasma radius can be significantly larger than the torque due to the NTV offset rotation profile, T_0^{NTV} , measuring this profile in these conditions is subject to error. Such plasmas can also have significant intrinsic rotation, V_i , from other sources which must be handled in the analysis. Analysis has been conducted on DIII-D to best handle these significant sources of error in torque balance calculations of the intrinsic rotation. Non-NTV-induced intrinsic rotation is found to be equivalent to the rotation driven by one full power neutral beam source [12]. Both experimental studies also introduce some element of modeling to describe an important component of the analysis, for instance, the NBI torque profile (which is not directly measured), or the solution of torque balance including both resonant and non-resonant magnetic braking. In addition, experimental research published to date has entirely focused on the ion channel providing the dominant drive for the NTV offset rotation, manifest by the models of the NTV offset rotation velocity, V_0^{NTV} , being proportional to $\sqrt{V_i}$. However, more complete NTV theory allows for torques generated by both the ion and the electron channels, the balance of which yields the total V_0^{NTV} profile [6,7].

3.1 Direct measurement of the NTV offset rotation profile

Recent experiments conducted on the KSTAR superconducting tokamak aimed to directly measure the V_0^{NTV} profile in plasmas not utilizing NBI heating, doing so for the first time in plasmas expected to have V_0^{NTV} dominated by the electron channel to more fully examine the theory. The experiment to directly measure the V_0^{NTV} profile utilized a simple approach. FIG. 3 illustrates the plasma current and line-averaged density used. Long pulse plasmas (up to 8s I_p flattop duration) allowed quasi-steady-state conditions to be produced, permitting two measurement times per plasma discharge. As discussed earlier, a prime objective of the experimental setup was to avoid the use of NBI to heat the plasma, as the co- I_p directed NBI system in KSTAR would also produce significant plasma rotation. Steady-state rotation speeds in an NBI heated plasma are expected to be approximately an order of magnitude larger than V_0^{NTV} , and so the use of NBI would obscure its measurement. Experiments were therefore conducted in plasmas heated ohmically, and also by the addition of up to 0.8 MW of

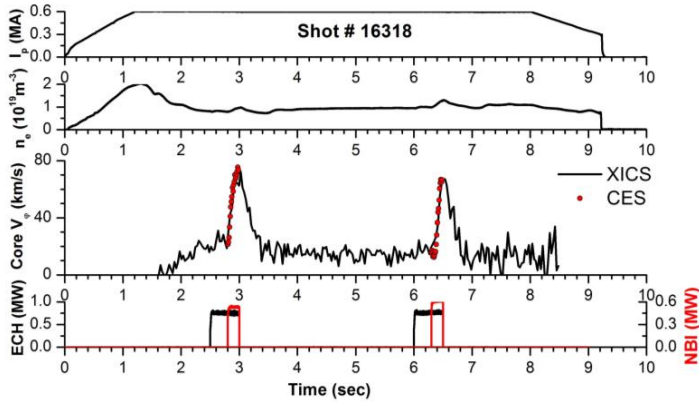


FIG. 3. Target plasma experimental setup for measurement of the NTV offset rotation profile (3D field not applied).

ion temperature profile measurement. FIG. 3 shows the relative timing of the ECH and NBI pulses, along with the core plasma rotation as measured by CES during NBI (in red). The measurement of V_0^{NTV} was made directly at the start of the NBI pulse, either using the earliest available measurement interval, or by making a small time extrapolation (~ 10 ms) back to the time at which NBI started (2.8s, 6.3s). An X-ray imaging crystal spectrometer (XICS) channel is shown along with the CES measurements in FIG. 3. Applied 3D fields were added to these plasmas to generate the NTV effect utilizing the KSTAR in-vessel control coils (IVCC) configured to deliver a predominantly $n = 2$ field. While measuring V_0^{NTV} , density feedback was utilized to maintain density control while 3D field strength was varied. To study its effect on V_0^{NTV} , variations to plasma temperature were also made by varying density at fixed applied 3D field strength.

The measurement of the V_0^{NTV} profile made here attempts to minimize error in the torque balance equation used to isolate it. Consider a simple and often-used torque balance equation (e.g. Eq. 8 of Ref. 12) $dL/dt = T_{NTV} + T_{NBI} + T_{ECH} + T_{Intrinsic} - L/\tau_{2D}$, where L is the plasma angular momentum, T_j terms are torques due to NTV, NBI, ECH, and a base “intrinsic” torque in an ohmic plasma, and τ_{2D} is the plasma momentum confinement time before the addition of the 3D field. We then consider a highly-simplified but often used expression for $T_{NTV} = C_1 \delta B^2 (V_\phi - V_0^{NTV})$, where δB is the magnitude of the applied 3D field. The

140 GHz second harmonic electron cyclotron heating (FIG. 3), as the strength of T_0^{NTV} theoretically depends strongly on plasma temperature. The plasma rotation profile was measured using charge exchange spectroscopy (CES) by utilizing a single NBI source running at somewhat derated voltages (50 – 60kV as opposed to normal operation at 90 – 95 kV) solely for the purpose of allowing plasma rotation and

multiplicative term C_I is known to be a function of plasma parameters, especially temperature [7]. Replacing L by IV_ϕ/R where I is the plasma moment of inertia, and considering that the intrinsic plasma rotation be considered as generated by the combination of T_{ECH} and $T_{Intrinsic}$, without any applied 3D field, the torque balance equation in terms of velocities is:

$$C_I \delta B^2 (V_\phi - V_{0-NTV}) + \frac{I}{R\tau_{2D}} (V_\phi - V_I) = 0$$

where V_I is the plasma intrinsic toroidal velocity profile due to all sources other than NTV. This equation elucidates the experimental approach to measure V_{0-NTV} . Clearly, when $\delta B = 0$, $V_\phi = V_I$ which is measured at the quasi-steady-states times 2.8 and 6.3s (FIG. 3). As δB is then increased, the plasma toroidal velocity profile begins to move away from V_I and toward V_{0-NTV} . With δB sufficiently large, V_ϕ approaches V_{0-NTV} and will saturate at that profile. The experiments followed this procedure and this expected dynamic was observed under various plasma conditions. An example is summarized in FIG. 4, which shows the measured V_I profile, and two profiles that saturate when the current, $I_{n=2}$, used to generate the applied $n = 2$ field reaches 3.2 kA/turn. Values of $I_{n=2}$ less than this value generated V_ϕ between these two profiles, which are omitted for clarity. The last two profiles in the scan of the applied 3D field are shown.

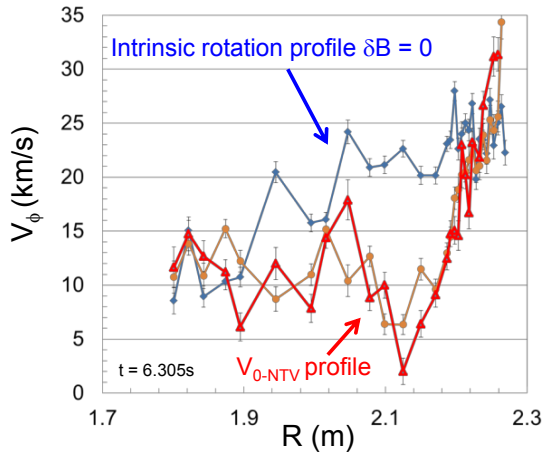


FIG. 4. Measured intrinsic rotation profile V_I , and saturated V_{0-NTV} profile in an EC heated plasma.

considered more generally, as the direction depends on the balance of the electron and ion non-ambipolar fluxes [6,7]. Being EC heated, the core plasma in FIG. 4 has (T_e/T_i) greater than 4, and the electron to ion NTV torque which scales as $(m_i/m_e)^{0.5}(T_e/T_i)^{3.5}$ indicates that the electron channel should be dominant, consistent with the co- I_p direction of V_{0-NTV} . Also, while the rotation in the plasma edge region, which equates to more than 12 krad/s, is not large compared to core V_ϕ values generated by NBI, it is quite significant compared to projections for ITER, which for a range of conditions are approximately 2 krad/s in the pedestal region [13]. Finally, the rotation shear that is generated in V_{0-NTV} is quite large – 15 times greater than the shear measured for the V_I profile shown.

3.2 Dependence of NTV offset rotation profile on temperature

Plasma conditions were varied to compare V_ϕ profiles under different heating conditions and to examine the effect of plasma temperature on the V_{0-NTV} profile. First, FIG. 5 shows a progression of V_ϕ profiles in ohmic plasmas, and an ECH plasma producing a V_{0-NTV} profile. First, the V_I profile (no applied 3D field) shown under ohmic conditions has V_ϕ near zero in the core region, increasing to about 7 km/s in the outer plasma. When the $n = 2$ applied field

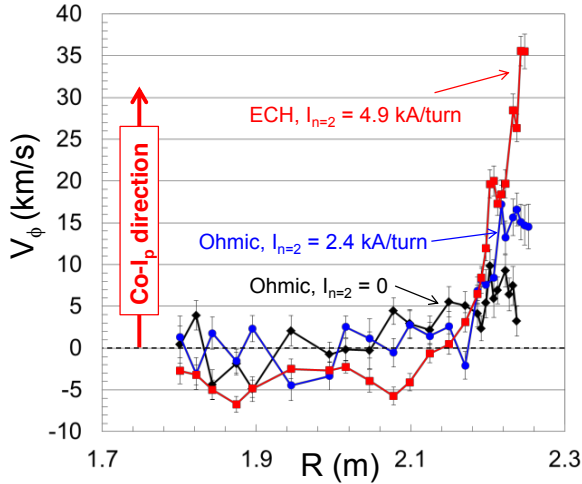


FIG. 5. Comparison of plasma rotation profiles in ohmic and ECH plasmas at varied 3D field levels.

now shows rotation in the counter- I_p direction as is expected if the NTV torque is dominated by the ion flux. This may be due to a higher density and somewhat lower (T_e/T_i) ratio in the core.

A comparison of V_{θ}^{NTV} profiles is shown for various plasma temperatures and constant $I_{n=2}$ in FIG. 6. The temperature variations were created by changing plasma density. The highest temperature plasma (the lowest density) yields a V_{θ}^{NTV} profile in the co- I_p direction in both the

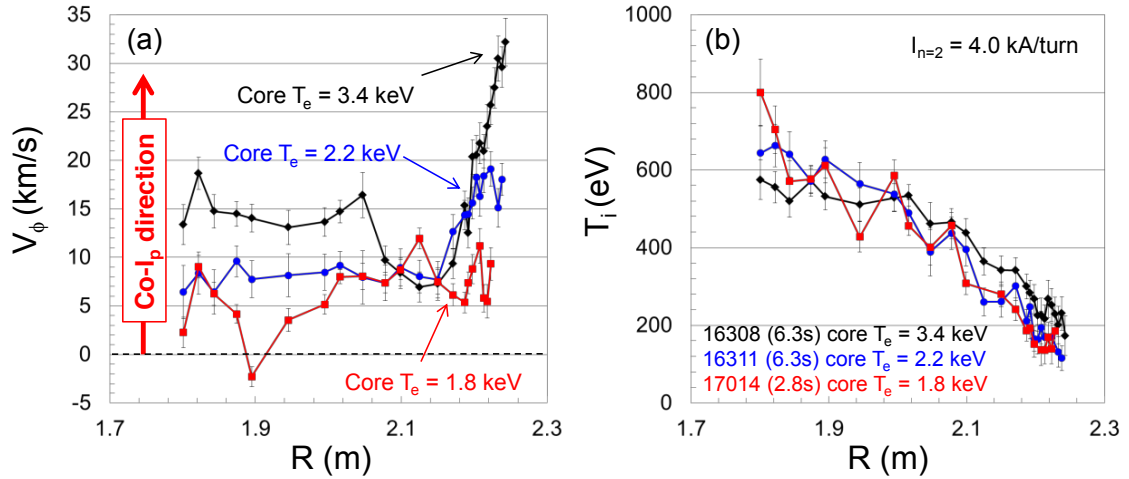


FIG. 6. (a) V_{θ}^{NTV} profiles at different plasma temperatures, and (b) T_i profiles for these variations.

core and outer region, with strong rotation shear in the outer region. The middle temperature produced with a line-averaged density feedback setting of $1.5 \times 10^{19}/\text{m}^3$ has decreased rotation in the core and outer regions. The lowest temperature had density set to $2.0 \times 10^{19}/\text{m}^3$ and V_{ϕ} in the outer region has dropped to levels found in the lowest rotation ohmic plasma in FIG 5.

Separate from the measurement of V_{θ}^{NTV} , an observation of the toroidal rotation profile evolution during the period of NBI heating in FIG. 3 shows that the effects observed are not caused by the heating systems alone, and have NTV characteristics. Most striking is the behavior of the plasma rotation when both the ion temperature and applied 3D field are

is added, (at somewhat smaller than the level needed to saturate the V_{ϕ} profile at V_{θ}^{NTV}), the V_{ϕ} in the outer region approximately doubles to 15 km/s. This shows that this rise is due to the application of the 3D field, and not simply due to a mechanism of the ECH. However, when ECH is added, the heating in the outer region apparently leads to a strong increase of V_{ϕ} , again more than doubling it to 35 km/s. This profile has increased $I_{n=2}$ to levels that saturate the rotation profile, producing the V_{θ}^{NTV} profile. In this case, while the characteristic strong co- I_p rotation is found in the outer region, the core region

sufficiently high. In plasmas where no 3D field is applied, once the NBI is turned on, the plasma expectedly spins up in the direction that the beam is injected. This is obvious for instance in FIG. 3 and is completely intuitive. However, as seen in FIG. 7, at $I_{n=2} = 4$ kA/turn,

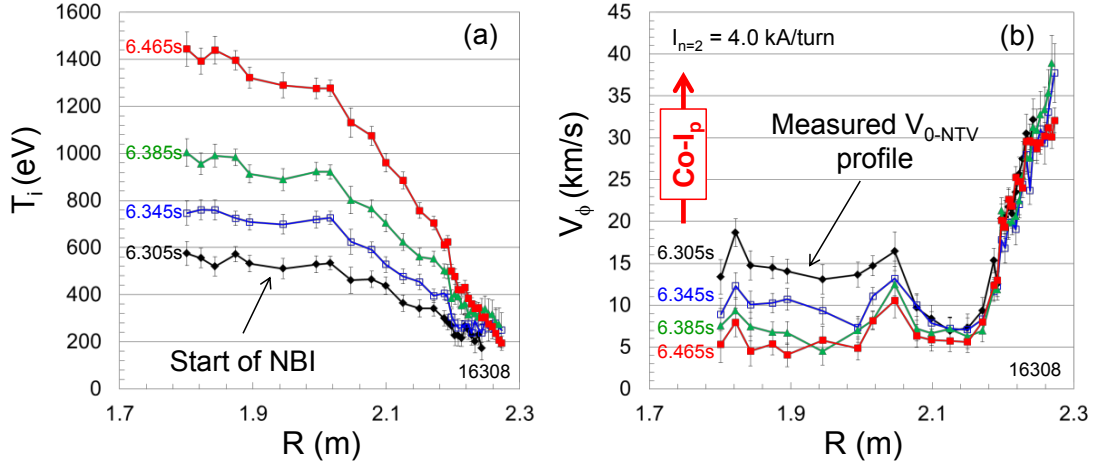


FIG. 7. Unintuitive observation of the plasma rotation profile moving in the direction opposite of an injected neutral beam when the plasma has sufficient temperature and applied 3D field strength.

the evolution of the V_ϕ profile away from the V_0^{NTV} profile is in the direction *counter* to the injected beam. Other examples at slightly lower $I_{n=2}$ show that the V_ϕ profile first increases in the direction of the injected beam, and later *reverses* direction and moves in the direction *counter* to the injected beam as the plasma ion temperature increases. Note that no MHD modes are observed, and there is no evidence of conventional mode locking in this case. This unintuitive result can be understood by a change in the T_{NTV} which typically increases with ion temperature, or a change in the V_0^{NTV} profile itself due to the temperature change.

This research was supported by the U.S. Department of Energy under contracts DE-FG02-99ER54524 and DE-AC02-09CH11466.

-
- [1] SHAIN, K.C., Phys. Plasmas **10** (2003) 1443.
 - [2] ZHU, W., SABBAGH, S.A., BELL, R.E., et al., Phys. Rev. Lett. **96** (2006) 225002.
 - [3] BERKERY, J.W., SABBAGH, S.A., BETTI, R., et al., Phys. Rev. Lett. **104** (2010) 035003.
 - [4] SABBAGH, S.A., BERKERY, J.W., BELL, R.E., et al., Nucl. Fusion **50** (2010) 025020.
 - [5] LIANG, Y., KOSLOWSKI, H. R., THOMAS, P. R., et al. Nucl. Fusion **50** (2010) 025013.
 - [6] SUN, Y., LIANG Y., SHAIN, K.C., et al., Nucl. Fusion **52** (2012) 083007.
 - [7] SHAIN, K.C., IDA, K., SABBAGH, S.A., Nucl. Fusion **55** (2015) 125001.
 - [8] GOUMIRI, I.R., ROWLEY, C.W., SABBAGH, S.A., Nucl. Fusion **56** (2016) 036023.
 - [9] SHAIN, K.C. and SABBAGH, S.A., Phys. Plasmas **23** (2016) 072511.
 - [10] GAROFALO, A.M., BURRELL, K. H., DEBOO, J. C., et al., Phys. Rev. Lett. **101** (2008) 195005.
 - [11] NOWAK, S., LAZZARO, E., SAUTER, O. et al., Journal of Physics Conf. Series **401** (2012) 012017.
 - [12] SOLOMON, W.M., BURRELL, K.H., GAROFALO, A.M., et al. Phys. Plasmas **17** (2010) 056108.
 - [13] POLEVOI, A.R., SHIMADA, M., SUGIHARA, M., et al. Nucl. Fusion **45** (2005) 1451.